Front. Chem. China 2010, 5(3): 247–261
DOI 10.1007/s11458-010-0002-2

FEATURE ARTICLE

Bioinspired synthesis and preparation of multilevel micro/nanostructured materials

Nü WANG[1], Yong ZHAO (✉)[2] and Lei JIANG (✉)[1,2]

1 School of Chemistry and Environment, Beijing University of Aeronautics and Astronautics, Beijing 100191, China
2 Beijing National Laboratory for Molecular Sciences (BNLMS), Key Laboratory of Organic Solids, Institute of Chemistry, The Chinese Academy of Sciences, Beijing 100190, China

In this review, some living organisms with multilevel hierarchical micro/nanostructures and related special properties are briefly introduced. The unique properties of organisms are mostly related to their special hierarchical micro/nanostructures. Inspired by nature, many zero-dimensional and one-dimensional micro/nanomaterials with biomimic or bioinspired multilevel micro/nanostructures have been successfully synthesized and prepared in recent years. Compared with traditional solid materials, the synthesis and preparation of these multilevel structured materials is more ingenious. Moreover, these kinds of multilevel micro/nanomaterials show fantastic properties in many fields because of their micro/nanoscale complex interior structures, which may be intended for application in catalysis, Li-ion batteries, biomedicines, sensors, and others.

Keywords biomaterials, micro/nanostructure, superhydrophobic, nanoparticles, nanotubes

1 Introduction

Creating high-performance functional materials is an eternal project of mankind. In this aspect, lives in nature have synthesized all kinds of biomaterials that have achieved almost all the processes of intelligence through long-term evolution. Therefore, learning from nature should be a more effective avenue in the development of smart materials [1]. Inspired by organisms in nature, we can mimic special functions of organisms from certain aspects to design and fabricate smart materials. As a result, we may eventually exceed nature in some aspects [2].

Scientific problems related to hierarchical complex structures in life exist everywhere. For example, the self-cleaning effect of lotus leaves [3], the anisotropic de-wetting behavior of rice leaves and wings of butterflies [4], the superhydrophobic force exerted by a water strider's legs [5], the unusual attachment mechanism of geckos [6], the antireflection property of some insect wings and eyes [7,8], and many others result from the special micro/nanostructures of the surfaces. Therefore, many bioinspired, multilevel structured materials are attracting more and more interest because of their unique properties [9–12]. In the past several decades, various special structured micro/nanomaterials with desired electronic, optical, magnetic, catalytic, and mechanical properties have been intensely investigated [9,12]. Why do so many scientists have a strong interest in multilevel structured micro/nanometer-scale objects? The reasons are considerably important. First, it is very helpful to deepen the comprehension of the micro/nanostructural formation mechanisms, which will give us inspiration in designing novel structured materials [13–21]. Second, the microscopic interior spaces and multiphase interfaces might lead to wonderful variations in the physicochemical properties compared with traditional bulk materials [16,19,21]. Third, the complex interior structures will enable us to better control the local chemical microenvironment that can bring many potential applications [22,23]. Here, we will mainly focus on the synthesis and preparation of hierarchical zero-dimensional (0D) and one-dimensional (1D) micro/nanomaterials.

In this review, we will give a brief introduction to the special structures and properties found in biologic systems. In the following sections, we will discuss the bioinspired

Received December 22, 2009; accepted January 29, 2010
E-mail: jianglei@iccas.ac.cn, zhaoyong@iccas.ac.cn

synthesis and preparation of 0D and 1D micro/nanomaterials with multilevel structures in the past few years; some representative applications of these novel materials will be presented. Lastly, we will give some personal opinions and outlook on these various multilevel structural materials.

2 Unique structures and properties in biologic systems

The special micro/nanostructures of organisms can generate special surface properties. For example, the self-cleaning property of some plant leaves (lotus leaves) and insect wings (cicadas, dragonflies, butterflies etc.) [4,24] results from the special microstructures on the surface. On these surfaces, there is a thin air layer trapped between the solid and water which can prevent water from wetting the surface; as a result, they exhibit superhydrophobic properties [25,26]. Theoretical studies show that the critical value of distance between two microstructures to generate superhydrophobicity is 100 nm, which has been verified by studies on the superhydrophobic property of a mosquito's compound eye. Moreover, some surfaces of natural materials such as rice leaves, the feathers of ducks and geese, as well as butterfly wings, etc., show the anisotropic sliding property of water droplets. That is, the rolling behavior of water droplets in the parallel and vertical direction is quite different, which is determined by the arrangement of the surface microstructure [27,28]. In addition, the antireflection properties of some insect wings and eyes also results from the special microstructures of the surfaces [7,8]. Other specific functions of organisms, such as water striders walking on water [29], geckos, spiders and flies being able to adhere to smooth walls and glass or even on ceilings [30,31], desert beetles collecting fog [32], beetles changing their color [33], and so on, are also closely related to their special surface microstructures.

2.1 Special surface properties

Many leaf surfaces of plants are water-repellent, and display a high self-cleaning ability. The leaves of *N. nucifera* afford an impressive demonstration of this effect, which is called the "Lotus Effect" (Figure 1(a)). Barthlott and Neinhuis first reported that this unique property is based on the coexistence of surface roughness caused by micrometer-scale papillae and the epicuticular hydrophobic wax [24,34]. Jiang et al. revealed that a superhydrophobic surface with both a large contact angle and small sliding angle needs the cooperation of nano and microscale structures. Figure 1(b) shows a typical

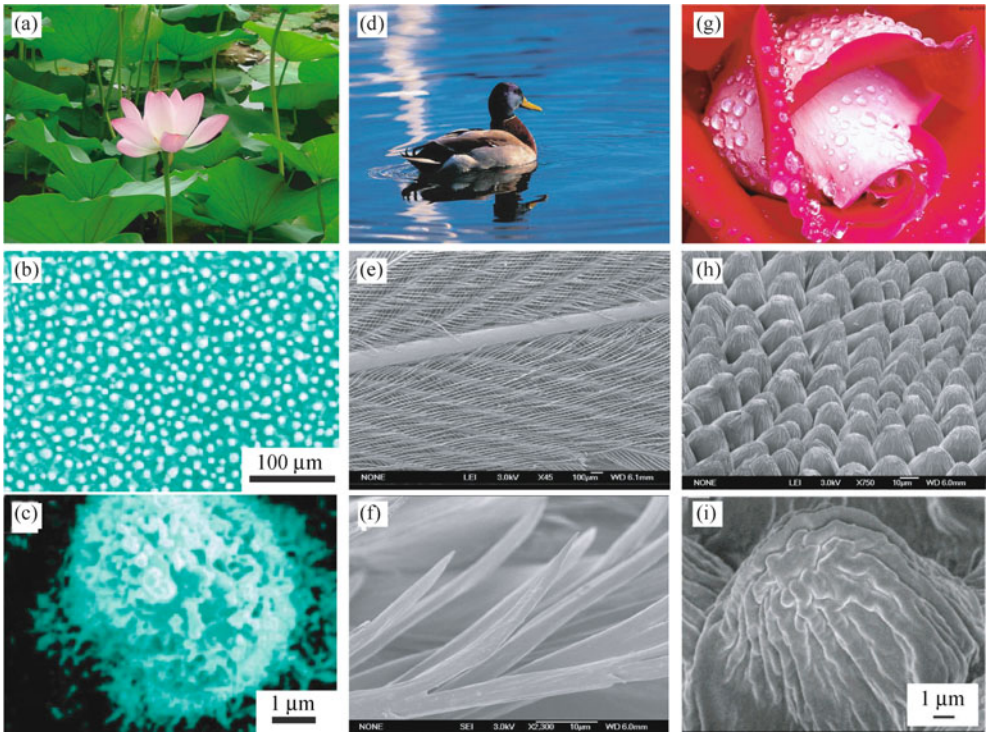

Figure 1 Self-cleaning property of some natural surfaces. (a), (d) and (g) show photographs of the three kinds of natural material, a lotus leaf, duck feather, and a rose, respectively. (b) and (c): SEM images of the surface of a lotus leaf [4]. Copyright Wiley-VCH Verlag GmbH & Co. KGaA. Reproduced with permission. (e) and (f): SEM images of a duck feather. (h) and (i): SEM images of a red rose petal. Reprinted with permission from Ref. [35]. Copyright 2008 American Chemical Society.

large-scale scanning electron microscopy (SEM) image of the surface of a lotus leaf on which many submicrometer papillae are found. Figure 1(c) shows a high-resolution SEM image of a single papilla, on which hierarchical structures in the form of branch-like nanofibers are clearly observed.

Anisotropic wetting and dewetting are also very important properties on patterned surfaces and have recently attracted much interest. It has been found that the arrangement of the microstructures on this surface can influence the way that a water droplet tends to move [4]. Jiang et al. found a sliding anisotropy tendency on the surface of a rice leaf [4]. Further, the feathers of some water birds like geese and ducks (Figure 1(d)) also show a sliding anisotropy when water drops roll off the feathers [27]. This waterproof function is attributed to the micron/sub-micron well-ordered strip-shaped structures of their feathers (Figure 1(e) and 1(f)). These kinds of structures help feathers have good hydrophobicity and air permeability. Furthermore, such well-ordered microstructures have the function of directional water-repellency so that water droplets can roll along the outer side of strips easily instead of wetting the bird's body.

In 2008, Feng et al. [35] studied hierarchical micropapillae and nanofolds existing on the petal surfaces of red roses (Figure 1(g)). They revealed that these micro- and nano-structures provide a sufficient roughness (Figure 1(h) and 1(i)) for superhydrophobicity and yet at the same time a high adhesive force with water which can be defined as the "petal effect."

The structure of some insects' compound eyes makes them have anti-reflecting characteristics. According to prior research, the compound eyes of moths consist of ordered hexagonal nanostructure arrays. These arrays are considered as the homogeneous transparent layer of the corneal surface. The low reflection generated by the protrusive nanostructures of a moth's eyes makes the moth seem to have abnormal inkiness and be less visible to predators even if it flies in the evening, which is called the "moth eye effect." A study found that a butterfly's cornea also has a similar structure to that of the moth [8]. Furthermore, different kinds of butterfly compound eyes have different sizes, resulting in differences in the degree of surface anti-reflectivity, such that the larger the height of the nanostructure, the lower the surface reflectivity. Recently, Yang and Jiang et al. discovered that the eyes of the mosquito also have excellent superhydrophobicity and antifogging properties [26]. This characteristic allows mosquitoes to maintain clear vision in a damp environment. These double characteristics are generated by micronipples and the hexagonally close-packed nanostructures on the micronipples (Figure 2(a)–(c)).

The water strider *Gerridae* is a kind of small insect that usually resides on the surface of ponds, slow streams, and marshes. In 2004, Jiang et al. revealed the secret of the water strider standing effortlessly and, in essence, walking quickly on the water surface [29]. They proposed that the special micro/nano-hierarchical structures of the legs are very important in inducing the superior water resistance (Figure 2 (d)). High resolution SEM observation indicates that there are numerous oriented tiny micrometer-scale needle-shaped setae covering the legs (Figure 2(e)). Moreover, many elaborate helical nanoscale grooves are found on each microseta, forming the unique hierarchical structure (Figure 2(f)). Air is thereby trapped in the spaces of micrometae and nanogrooves to form an air cushion at the leg-water interface that prevents the legs from being wetted. Therefore, the water strider can move quickly on the water surface without wetting its legs, and the superhydrophobicity of the legs is presented in macroscopic view. This discovery can be helpful in producing new waterproof materials. More importantly, it may shed light on the design of new aquatic microdevices. Zhang et al. [36] from Tsinghua University reported a method for the fabrication of floating superhydrophobic gold thread to mimic the legs of water striders by combining the layer-by-layer self-assembly technique and electrochemical deposition of gold aggregates. Shi et al. [37] from Tsinghua University also reported a simple route for producing copper wire with superhydrophobic submicrofiber coating to mimic the legs of water striders. This research may open new and promising applications for biomimetic drag-reducing and quick propulsion techniques. It is a typical example of the combination of learning from nature and exceeding it.

Geckos are well-known for their unique ability to climb rapidly up smooth vertical surfaces, even adhering to ceilings upside down (Figure 2(g)). In 2000, Full et al. revealed the mechanism of the high adhesive force of geckos' feet [30]. They considered that the special high adhesive force was an accumulation of van der Waals forces between the numerous hairs on the feet of geckos and surface molecules of the solid materials. The van der Waals force is a weak attractive or repulsive electromagnetic force between close contact neutral molecules. The van der Waals force is so weak that it is usually neglected when studying the mechanism of high adhesion. Therefore, the relationship between this molecular scale force and the gecko's adhesion seems unacceptable. Microscopy shows that there are nearly five hundred thousand keratinous hairs or setae on a gecko's foot (Figure 2(h)). Each hair is about 100 μm long, and contains 400–1000 fine terminal branches called spatulae (Figure 2(i)). For the hierarchical fine structures, the distance between the surface molecules and the setae becomes much closer, and the van der Waals force works. Although the force generated by each single hair is negligible, the accumulation of the force from thousands of setae becomes strong enough to support the body of the gecko.

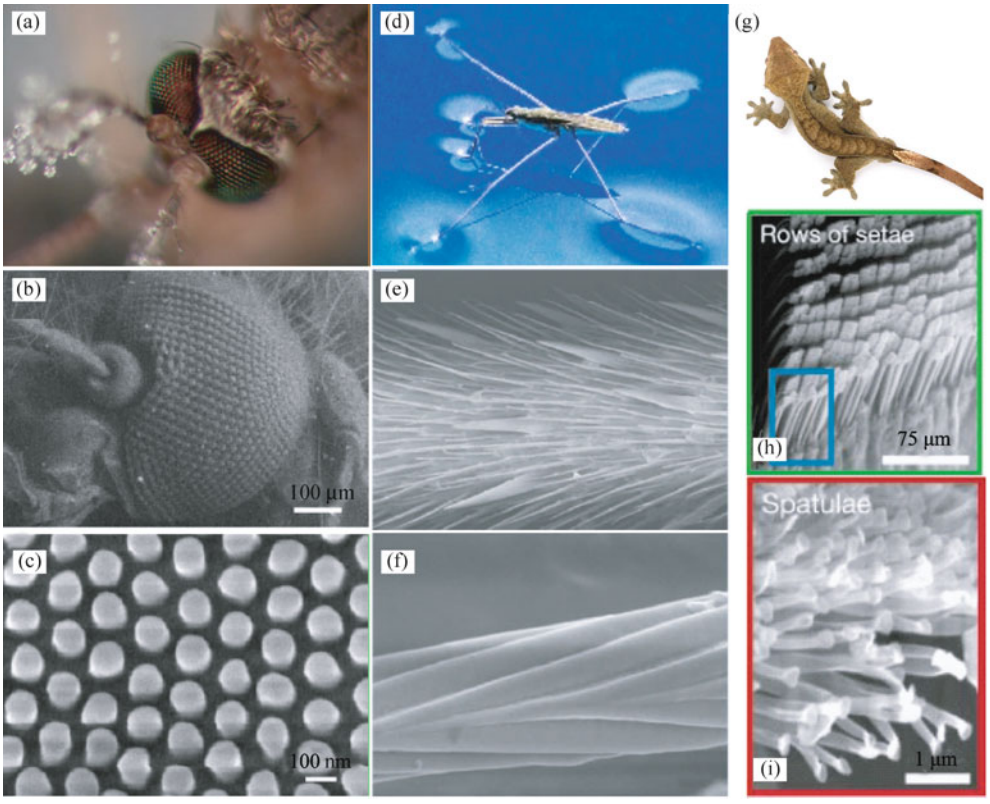

Figure 2 (a) photograph of a mosquito eye. (b) and (c) SEM images of a mosquito eye [26]. Copyright Wiley-VCH Verlag GmbH & Co. KGaA. Reproduced with permission. (d) photograph of a water strider. (e) and (f) SEM images of microsetae. Scale bars: (e) 20 μm; (f) 200 nm. Reprinted with permission from Macmillan Publishers Ltd: [Nature] (Ref. [29]), copyright 2004 Nature Publishing Group. (g) photograph of a gecko. (h) and (i) SEM images of setae. Reprinted with permission from Macmillan Publishers Ltd: [Nature] (Ref. [30]), copyright 2000 Nature Publishing Group.

2.2 Structural color of organisms

Peacock feathers, some beetles, butterfly wings, natural opals, pearls, etc., are of colorful appearance not because of chemical dyes or pigments but due to structural color (Figure 3(a) and 3(c)) [38–43], which is caused by microstructures that exhibit periodic variations in one, two, or three dimensions (Figure 3(b) and 3(d)). Most natural materials with structural color consist of photonic crystals [44,45], but the molecular structure, micro/nanostructure, periodic structure and function of these photonic crystals has still not been very clear up to now. Thus, studies on the color of organisms, particularly on the photonic crystals related to structural color, should play an important guiding role in the development of a new generation of photonic materials, storage materials and display materials.

2.3 Advanced optical system

Generally, photosensitivity in most echinoderms is attributed to "diffuse" dermal receptors. However, the latest research shows that brittlestars (*Ophiocoma wendtii*) can change color from day to night (Figure 4(a)) as certain single calcite crystals used by brittlestars for skeletal construction are also a component of specialized photosensory organs, conceivably with the function of a compound eye [46]. An analysis of arm ossicles in different kinds of brittlestars showed that in light-sensitive species, the periphery of the labyrinthic calcitic skeleton extends into a regular array of spherical microstructures that have a characteristic double-lens design (Figure 4(b)). The SEM of the cross-section of a fractured dorsal arm plate from *Ophiocoma wendtii* shows that the peripheral layer consists of calcitic stereom and the enlarged lens structures (Figure 4(c)). Further investigation of the cross-section of an individual lens shows that the operational part of the calcitic lens closely matches the profile of a compensated lens. These results represent an example of a multifunctional biomaterial that fulfills both mechanical and optical functions.

The polar bear is white in appearance, but its skin is actually dark green [47]. The polar bear's fur has excellent ability to absorb infrared light, thus exhibiting excellent thermal insulation performance (Figure 4(d)). The SEM

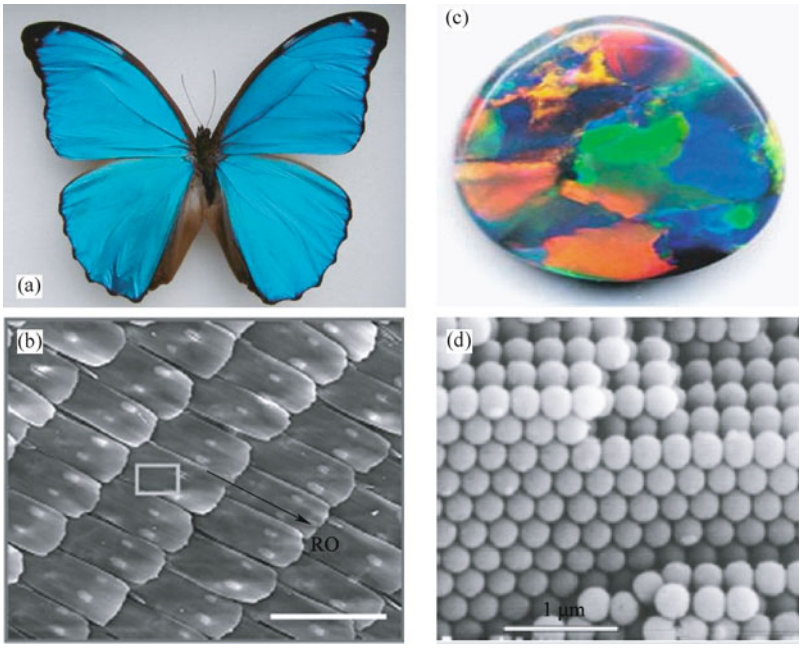

Figure 3 Structural color of organisms: butterfly wings (left) and natural opals (right). (a) and (c) photographs. (b) [28] (Reproduced by permission of The Royal Society of Chemistry) and (d) (http://nano.nchc.org.tw/photonic/ch1.php) SEM images. Scale bar: (b), 100 μm.

image indicates that the fur of polar bears is colorless hollow tubes (Figure 4(e)), and optical observations show that the diameter of these tubes becomes larger and larger gradually from the end to the root (Figure 4(f)) [48]. The reason why polar bear fur looks white is the rough inner surface of the fine tubes which causes the diffuse reflection of light. This unique structure and color of the polar bear results from its long-term struggle against an extremely cold environment. Therefore, scientists have envisaged that if artificial hollow fibers with thermal insulation and efficient energy-saving performance could be fabricated by mimicking the structure of polar bear fur, the utilization of solar energy could be greatly improved, which would be immeasurably beneficial to human beings. Much interest has been aroused in the fabrication of multichannel tubular structures for their outstanding performance, however, the question of how to fabricate such multichannel micro/nanotubes is still a challenge.

2.4 Other special properties related to multilevel structure

Many biologic systems with outstanding properties have self-assembled hierarchical structures over multiple scales, such as the polar bear's fur mentioned above, and have multiscale structures which lead to the outstanding performance and versatility. Similar to the polar bear's fur, feathers of many birds also have this extremely elaborate multichannel and multichamber tubular structure, as shown in Figure 5(a) [49]. This delicate structure can greatly reduce the weight of feathers and serve as heat-shields on the basis of maintaining enough mechanical strength, by which birds can fly in the sky with light feathers.

On the other hand, these kinds of multiscale structures of biologic materials also have special deformation characteristics. For example, pine has rectangular type cells and round type pits (Figure 5(b) and 5(c)) [50]. They have 50–100 μm cells, which are connected with 5–20 μm pits. Such a hierarchical structure can make its response to stress like that of a spring [50,51]. Influenced by the polymer matrix consisting of hemicellulose and lignin, the hard cellulose fibers couple with each other in a tangential direction and the soft matrix on the interface controls the whole deformation process of the wood cell wall.

Researchers have observed the surface structure of a mature sea urchin spine by SEM [1]. The ideal multilevel structure is also an inartificial porous single crystal which is a composite of organic macromolecules and oriented $CaCO_3$. This gives us bio-inspiration on how to design and synthesize hierarchical structures.

In brief, many unique properties in biologic systems are attributed to their hierarchical structures. Some ingenious functions in organisms are far smarter than human design. Learning from intelligent materials in nature provides an effective way of designing bio-inspired materials, and lays a bridge between biology and other scientific subjects. Based on

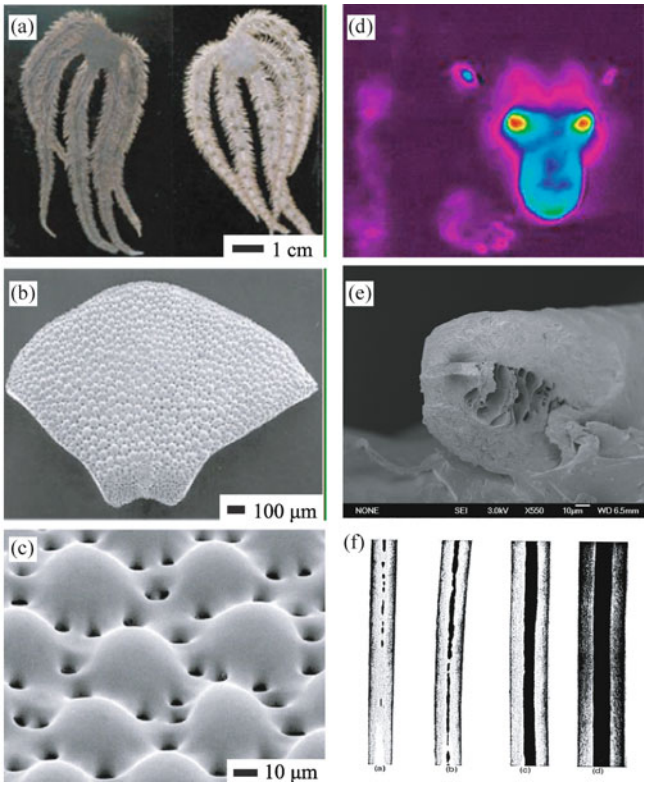

Figure 4 (a) Lightsensitive species O. wendtii changes color markedly from day (left) to night (right). (b) SEM of a dorsal arm plate (DAP) of O. wendtii cleansed of organic tissue. (c) SEM of the peripheral layer of a DAP from O. wendtii with enlarged lens structures. Reprinted with permission from Macmillan Publishers Ltd: [Nature] (Ref. [46]), copyright 2001 Nature Publishing Group. (d) photograph of polar bear under infrared night vision. (e) and (f) microstructure of the polar bear's hair. (e) cross section image. (f) vertical image [48]. Copyright Optical Society of America.

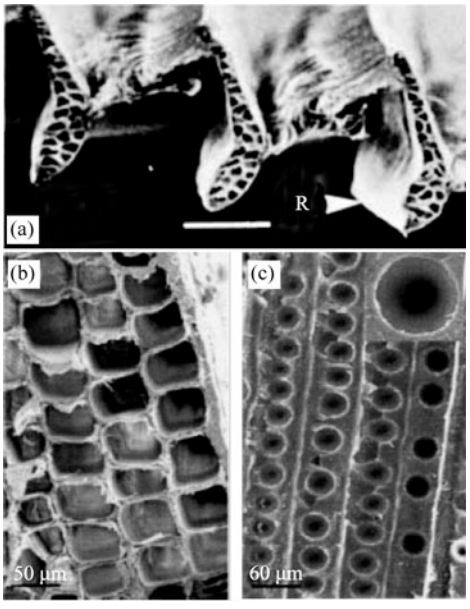

Figure 5 (a) Transverse sections of rami of remiges of *Nothoprocraperdicaria*. Scale: 100 μm [49]. Copyright Wiley-VCH Verlag GmbH & Co. KGaA. Reproduced with permission. (b) and (c) SEM images of dry wood (b) pine (cross-section), (c) pine (radial) [50]. Copyright Wiley-VCH Verlag GmbH & Co. KGaA. Reproduced with permission.

the correlation between properties and multilevel structures of natural materials, artificial novel materials with similar properties and structures could be designed.

3 Micro/nanomaterials with multilevel structure

3.1 Zero-dimensional multilevel structured micro/nanomaterials

The synthesis and preparation of 0D particles and spheres has experienced a structural evolution from simple to complex owing to the development of modern synthetic technology and analytical instruments. Accordingly, many kinds of 0D micro/nanomaterials with multilevel structures have been successfully fabricated, such as porous spheres, rattle spheres, multichamber spheres and so on.

Porous spheres are microspheres saturated with micrometer to submicrometer pores. Compared with traditional solid materials, these kinds of porous structure spheres have more specific surface areas and are less dense, and are regarded as a microspherical sponge. Nowadays, the emulsion route is recognized as an effective way to fabricate macroporous structure spheres [52–59]. Ma et al. have developed a membrane emulsification technique to prepare polymer macroporous microspheres [56–59]. In this technique, one kind of liquid phase (oil) was introduced into another immiscible liquid phase (water) through a porous membrane. The oil which passed through the membrane was broken up into microdroplets and then was dispersed into the water to form an oil-in-water emulsion. This method can generate a uniformly sized porous polymer leading to many polymers which can easily dissolve in the oil phase. Ma et al. synthesized various porous poly(styrene-divinyl benzene) microspheres by this method, as shown in Figure 6(a) [58].

Yang et al. have prepared colloidal particles of complex structures using oil-in-water emulsion droplets as confined geometries which are shown in Figure 6(b) [60]. Ge et al. have designed and fabricated cage-like polymer microspheres with a hollow porous shell structure (Figure 6(c) and 6(d)) by combining the emulsion method and template method [52].

Another effective way to fabricate porous spheres is by spray methods, including electrospray techniques and the pressure spray drying method. The electrospray technique is an electrohydrodynamic process supplied with a high voltage.

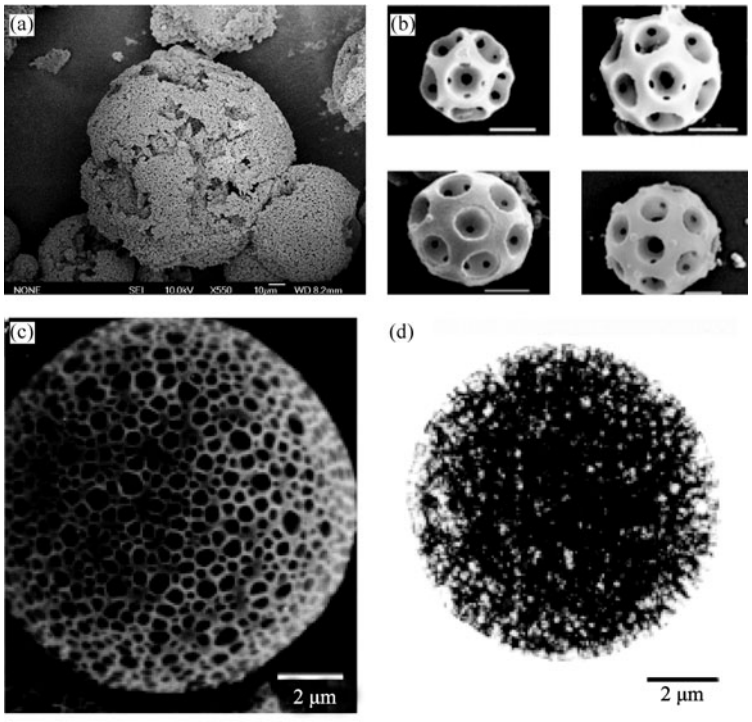

Figure 6 (a) SEM image of the microspheres. Reprinted from reference [58], copyright 2007 with permission from Elsevier. (b) Cage like porous silica particles. Scale bars are 1 μm. Reprinted with permission from Ref. [60]. Copyright 2007 American Chemical Society. (c) and (d) SEM and TEM micrographs of PVA microspheres. Reprinted with permission from Ref. [52]. Copyright 2005 American Chemical Society.

The conductive liquid is pumped through a nozzle to form an electrically charged jet of solution owing to electrostatic repulsions. The solution jet solidifies with accompanying evaporation of solvent and forms a film on the collector. This method is widely employed to generate micro/nanoparticles. Jiang et al. have fabricated polystyrene (PS) porous microparticles with variable morphologies by electrospray [61]. Figure 7(a) and 7(b) show the PS particles prepared from 5% and 7% by mass PS/DMF solutions respectively. It is obvious that the morphologies of the particle are quite different. Consequently, this means that the morphologies of the electrospray particles could be controlled by varying the concentration of the solution. Han et al. have studied various morphologies of the PS surface affected by the solution properties and electrospray conditions [62]. Furthermore, some porous microspheres have also been successfully prepared by the spray drying method. This method often involves three parts: template filing, figuration, and template removing. Li et al. have reported highly ordered porous photonic balls composed of titania framework which were fabricated by using a titania precursor templated around PS photonic balls (Figure 7(c) and 7(d)) [63]. In addition, Yan et al. have reported a vivid hierarchical self-assembly on the mesoscopic scale in the preparation of a new class of giant large compound vesicles [64].

The most direct applications of multilevel micro/nanostructured materials are in catalysis, as a result of the high specific area and multiphase heterogeneous interfaces. Okuyama et al. have fabricated macroporous brookite TiO_2 microspheres by spray drying a TiO_2 nanoparticle suspension, showing improved photocatalytical properties compared to same sized solid counterparts [65]. Zhai et al. hierarchically synthesized micro/nano-porous TiO_2 films which show that the catalytic activity was increased 30%–40% and 60%–70% for mineralizing gaseous acetaldehyde and liquid-phase phenol respectively [66].

Compared to the traditional core-shell structures in which the core and shell components are compactly attached without any interspaces, more and more scientists have begun to pay attention to the rattle spheres (or so-called yolk-shell hollow spheres) with a void intermediate layer [67–73]. Rattle sphere structures have one or several movable core particles which have been enclosed in a hollow sphere. It is a development of the ordinary core-shell structure. The template method can be regarded as a comparatively familiar way to synthesize this kind of structure [17,23,68,74–79]. This method can be summarized in three steps which are shown in Figure 8(a) [78]. First, the core-shell spheres are prefabricated with two

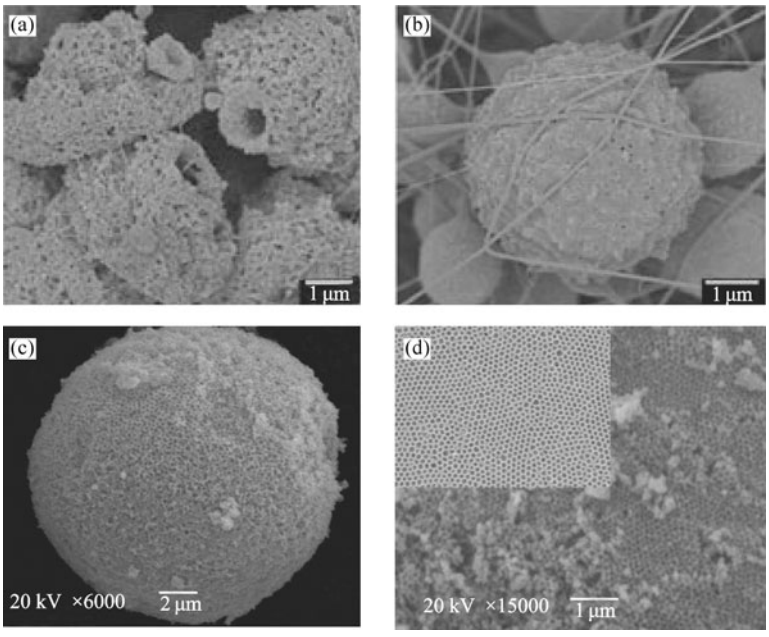

Figure 7 (a) and (b) SEM image of electrospun PS particles from 5% and 7% PS/DMF solution [61]. Copyright Wiley-VCH Verlag GmbH & Co. KGaA. Reproduced with permission. (c) Fractional section image of broken opaline balls. (d) Surface image of the inverse opaline balls [63]. Reproduced by permission of The Royal Society of Chemistry.

different substances which will serve as the template and core supplier. Secondly, the core-shell spheres are coated with a layer of the third substance by a physical or chemical method. An egg-like structure with a three-layered structure which is similar to a "yolk, egg white, and egg shell" is formed. When the "egg white" is selectively removed by an appropriate method, the novel core-shell spheres are then obtained. We will usually refer to this kind of structure as a yolk-shell structure here. Yang et al. demonstrated the template method for preparing hollow TiO_2 nanoparticles with movable silica nanoparticles inside (HTNMSNs). Figure 8(a) shows the procedure for preparing HTNMSNs. They used monodisperse silica-polystyrene core-shell nanospheres (SiO_2-PS-CSNs) sulfonated as templates. Then they prepared the composite shell consisting of TiO_2 and sulfonated polystyrene (SPS) through adsorbing or depositing of tetrabutyl titanate gel into the SPS shell. Finally, the HTNMSNs were obtained after all the polymers were removed by dissolution or calcination.

By using a similar technique, various rattle structured spheres have been prepared. For example, Shi et al. have synthesized hollow magnetic mesoporous spheres with Fe_3O_4 particles encapsulated in the core silica microspheres [68]. Yin et al. have fabricated homogeneous SiO_2@SiO_2 [80] and heterogeneous Au@SiO_2 [81] rattle structured spheres (Figure 8(b)), respectively. Tang et al. have prepared core-shell silica microcapsules which are shown in Figure 8(c) [76].

For inorganics, the Kirkendall effect and Ostwald ripening

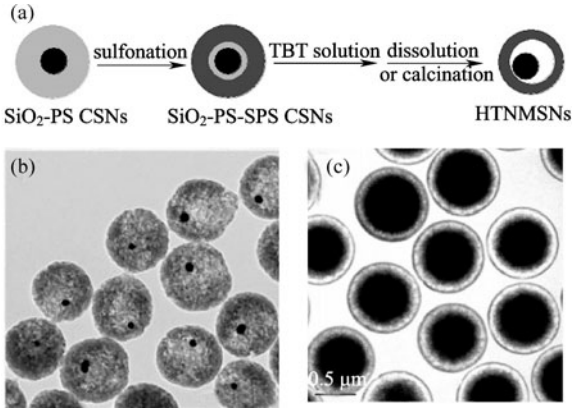

Figure 8 (a) Synthesis scheme for hollow titania spheres with movable silica spheres inside. Reprinted with permission from Ref. [78]. Copyright 2004 American Chemical Society. (b) TEM image of Au@SiO_2 core-shell particles, scale bar is 200 nm. Reprinted with permission from Ref. [81]. Copyright 2008 American Chemical Society. (c) TEM image of the core-shell silica microcapsules. Reprinted with permission from Ref. [76]. Copyright 2005 American Chemical Society.

mechanism are employed here to generate rattle structure materials. The Kirkendall effect refers to the different atomic diffusion rate between two coupled components. This diffusion difference will generate vacancies in the lower melting component side near the interface. In recent studies, scientists have begun to create hollow nanostructures using a nanoscale Kirkendall effect. Wang et al. have used a one step

self-templated synthetic route to fabricate various structured hybrid rare earth nanomaterials from hollow structured to core-shell structured to rattle structured by the Kirkendall hollowing effect [82]. Another important solution synthesis strategy to generate rattle structures is based on the Ostwald ripening mechanism. Ostwald ripening refers to growth in solution where larger crystals are from the smaller ones. A larger crystal is more energetically stable than the smaller one, so that molecules on the surface of small particles will diffuse and recrystallize on the surface of the larger particles in order to lower the total energy of the solution. It is a typical thermodynamically driven spontaneous process. Zeng et al. have prepared a series of yolk-shell structured inorganic semiconductor particles by Ostwald ripening [83,84].

Due to the hierarchical structure and various other components, rattle spheres have many potential applications in related fields. For example, lithium-ion batteries (LIBs) have attracted much attention in the scientific and industrial fields due to their high electromotive force and high energy density. The preparation of appropriate advanced electrode materials with multilevel micro/nanostructures is an important way to make materials with a higher energy density and more cycle characteristics. Cao et al. synthesized hollow multi-layered nanocrystalline SnO_2 microspheres (Figure 9(a) and 9(b)) by chemically induced self-assembly in a hydrothermal environment which exhibits good electrochemical performance as the anode material in LIBs [85]. Wan et al. have fabricated tin nanoparticles encapsulating elastic hollow carbon spheres worked as anode materials showing very high specific capacity and excellent cycling performance [23].

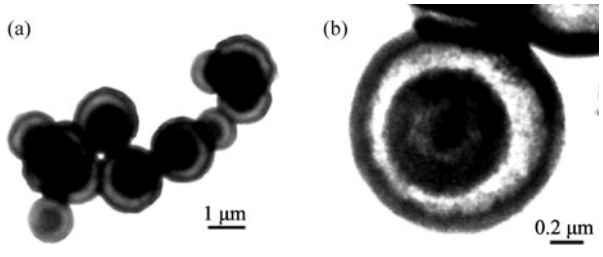

Figure 9 (a) TEM image of the HS-SnO_2. (b) The magnified image of a single HS-SnO_2. Reprinted with permission from Ref. [85]. Copyright 2007 American Chemical Society.

The multilevel micro/nanostructured interior materials are also widely used in biomedical areas. Shi et al. have successfully fabricated a novel kind of hollow rattle magnetic mesoporous sphere with Fe_3O_4 particles encapsulated in the cores of mesoporous silica microspheres [68]. Such structured spheres have obvious advantages both an enhanced drug-loading capacity and a significant magnetization strength. Xu et al. have demonstrated that a new type of multifunctional nanomaterial, FePt@Fe_2O_3 rattle nanoparticles, could be used as magnetic resonance imaging contrast and anticancer agent simultaneously [73].

More complex hollow spheres are multishell spheres which refer to particles consisting of multiple shells with different diameters which could be regarded as a nestification of several hollow spheres. Some scientists call them "onion" structures. The multishell spheres are usually synthesized by the template method and self-assembly approach. Traditional core-shell structured composite spheres are often prepared by coating against a solid spherical template. When the template core is removed, the hollow spheres are obtained. Thereby, it could be directly assumed that multishell spheres could be created when a hollow structured template instead of a solid spherical template is used. This method is easy in principle, but the practical preparation process is not an easy task. The selection of a suitable hollow structured template is the first difficult point. Second, it is difficult to deposit the desired materials onto the outer and inner surfaces of the hollow template simultaneously, especially on the inner surfaces. Though the process is complex, several kinds of multishell spheres have still been successfully synthesized by this method. Yang et al. have used hollow latex cages (HLCs) as templates to fabricate composite hollow spheres with complex structures [86]. The route of the synthesis process is shown in Figure 10(a) [86]. The template HLCs have a PS shell with transverse hydrophilic channels connecting to an interior hydrophilic surface. Following the first route, materials grew both onto the hydrophilic interior surface and with the channels, leading to hollow composite spheres. When the HLCs were removed by dissolution or calcination, hollow spheres were obtained. In the second route, composite spheres are used as templates to grow another material onto the exterior surface of the sphere, and sandwiched composite spheres are prepared. After removing the HLCs, double-shelled hollow spheres are obtained. Figure 10(b) and 10(c) show the TEM images and SEM images (inset) of double-shelled silica/titania composite hollow spheres formed by a silica sol-gel process onto the exterior surface of the titania composite spheres before and after the HLCs are dissolved, respectively.

Scientists have also used a normal solid template to fabricate multishell spheres indirectly. Wu et al. [87] have demonstrated the preparation for SiO_2/PS/TiO_2 multilayer core-shell hybrid microspheres. They first synthesized SiO_2/PS core-shell hybrid particles by cationic initiator emulsion. Then the SiO_2/PS core-shell hybrid particles were mixed with tetra-*n*-butyl titanate for the sol-gel reaction to directly form SiO_2/PS/TiO_2 multilayer core-shell hybrid microspheres. In some cases, the multishell structure and yolk-shell structure are combined when a solid core is wrapped in multishell hollow shells. Archer et al. have successfully synthesized

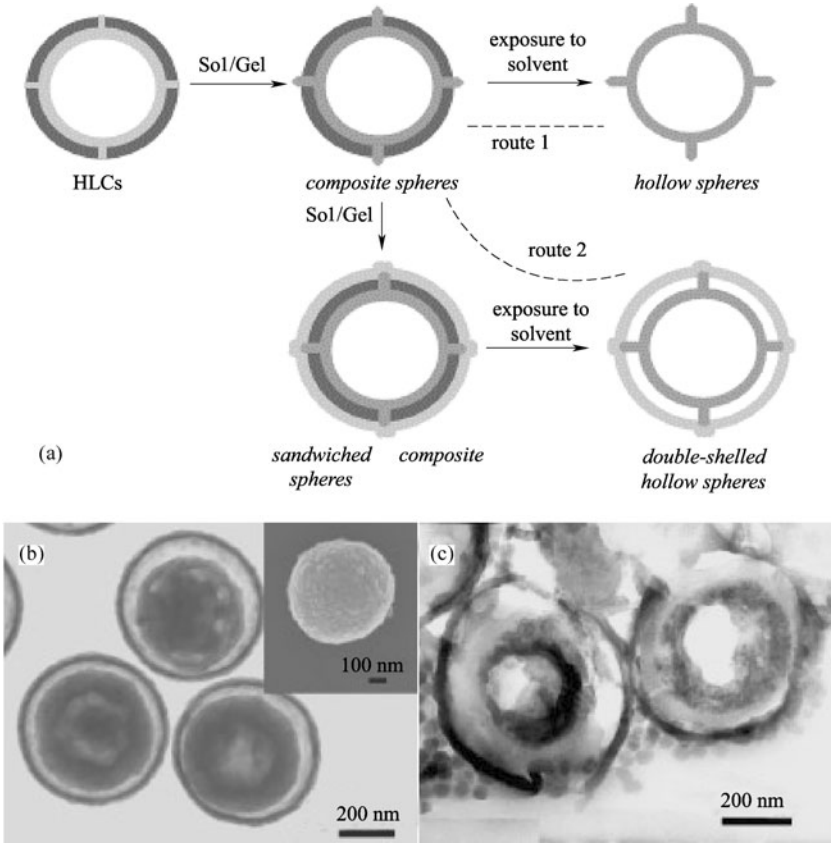

Figure 10 (a) Illustration of the template synthesis of composite spheres with complex structures [86]. (b) TEM image and SEM image (inset) of double-shelled silica/titania composite hollow spheres formed by a silica sol-gel process onto the exterior surface of the titania composite spheres. (c) TEM image of ultramicrotomed silica/titania composite hollow spheres (after HLCs were dissolved) [86]. Copyright Wiley-VCH Verlag GmbH & Co. KGaA. Reproduced with permission.

double shelled Au/SnO_2 hollow colloids in this strategy by shell-by-shell hydrothermal deposition on silica templates [88].

Chen et al. have prepared multilayered hollow microspheres from an amphiphilic pharmaceutical molecule, azithromycin, by using a simple self-assembly approach [89]. Figure 11(a) indicates the multistep build-up process controlled by a spatially periodic precipitation mechanism. Azithromycin is a kind of amphiphilic molecule that is soluble in ethanol but insoluble in water. When the ethanol solution with azithromycin is introduced to water, it first forms a suspension of numerous giant vesicles. Then, the azithromycin molecules diffuse outward with the ethanol due to the concentration gradient of the azithromycin solution from the inside of the vesicle to outside, in the bulk solution. The region near the surface of the vesicle may gain a higher concentration of azithromycin molecules (step 1 of Figure 11(a)). And then the azithromycin will precipitate to form the first layer, due to azithromycin being poorly soluble in mixtures with a high proportion of water (step 2 of Figure 11(a)). The precipitation process that formed the first layer results in local depletion of free azithromycin molecules. So, the precipitation process is temporarily terminated and a hollow intermediate layer formed. Subsequently, azithromycin molecules enveloped within the microsphere still diffuse outward, driven by the concentration gradient (step 3 of Figure 11(a)). Afterwards, the precipitation process will start once again (step 4 of Figure 11(a)). The cycle repeats itself until the concentration of azithromycin molecules is insufficient to provide the driving force for the precipitation of further layers. Therefore, it is possible to control the number of layers of this kind of multishell microspheres by manipulating the initial azithromycin concentration. Figure 11(b) and 11(c) show the optical microscopy image and SEM image of the morphology and structure of the multishell hollow microspheres from this method.

The sensitivity of sensors could be increased efficiently when incorporating the multilevel micro/nanostructured materials. Zhu et al. synthesized Cu_2O microspheres with multilayered and porous shells which could be used to fabricate a gas sensor, showing much higher sensitivity than solid Cu_2O microspheres [22].

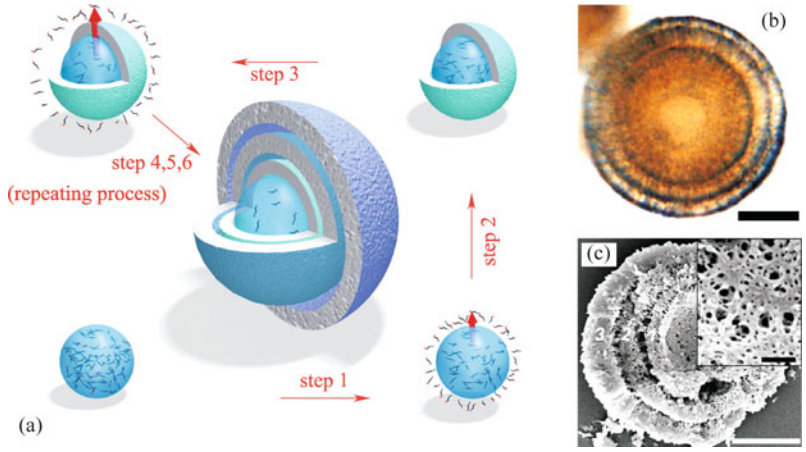

Figure 11 (a) Schematic illustration of the spatially periodic precipitation mechanism of the layer construction process. Step 1: diffusion process. Step 2: precipitation for layer construction. Step 3: repeated diffusion process. Step 4, 5, and 6: repeat of first three steps. (b) Optical microscopy image of a microsphere in suspension. (c) SEM image of a cross-section of a microsphere. The inset shows the detailed porous structure of the internal microsphere. Scale bars of (b) and (c) represent 10 μm [89]. Copyright Wiley-VCH Verlag GmbH & Co. KGaA. Reproduced with permission.

Multichamber spheres refer to the spheres with multiple distributed independent chambers. These chambers are separated from each other and so it can be assumed that it is difficult to precisely control the number of the inner chambers. Therefore, the reports about such multichamber spheres are quite few in number. Torii et al. have created microdroplets with multichambers by water-in-oil-in-water (W/O/W) or oil-in-water-in-oil (O/W/O) double emulsions using microfluidic systems [90]. Weitz et al. have presented a scalable microcapillary technique wherein the number and the size of the inner droplets are controlled with complex multiple emulsions [91]. It is notable that the multichamber spheres mentioned above are metastable, as most of them are liquid-in-liquid systems.

Recently, Zhao et al. reported a novel multifluidic compound-jet electrospray technique to fabricate multichamber microspheres in one-step. The number of chambers could be controlled by the number of inner capillaries [92]. Figure 12 (a) shows the set-up of the multifluidic compound-jet electrospray. Several metallic capillaries were embedded separately into a blunt metal needle to form a hierarchical compound nozzle, which was connected to a high voltage generator. The immiscible outer fluid and several kinds of inner fluids were respectively fed to the outer and inner capillaries in appropriate flow rates. The compound droplets solidified into multichamber spheres on the grounded substrate below with a suitable electric field. The number of obtained microspheres corresponds with the number of inner fluids. Figures 12(b)–(e) show the SEM images of the microspheres with a chamber number from one to four, respectively.

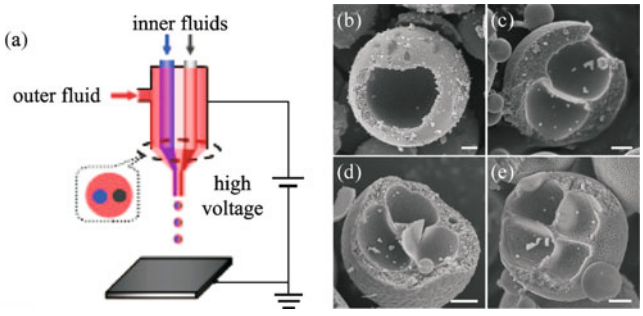

Figure 12 (a) Multifluidic compound-jet electrospray set-up. (b)–(e) Cross-section SEM images of titania microcapsule with welltailored one (b), two (c), three (d), and four (e) compartments, respectively. They correspond to the original compound nozzle with the same number of inner capillaries. Scale bar: 500 nm. Reprinted with permission from Ref. [92]. Copyright 2008 American Chemical Society.

3.2 One-dimensional micro/nanomaterials with multilevel structure

The 1D micro/nanomaterials that we discuss here can be similarly classified along with the 0D micro/nanomaterials mentioned above. They are bamboo-like tubes, wire-in-tubes, multiwalled tubes and multichannel tubes, respectively. Though the preparations of anisotropic 1D materials are more complicated than those of isotropic spherical 0D materials, some 1D multilevel structured micro/nanomaterials have been successfully generated by many ingenious approaches.

Bamboo-like tubes are a type of tubular microscopic material characterized by micro/nanotubes stuffed with

another substance or air which are like a miniaturized bamboo stem. Chen et al. have reported bamboo-like titania/silica hybrid nanotubes which contain linear mesocage arrays by a step-by-step hierarchical template method [14]. Directly utilizing the existing micro/nanotubes as a precursor is another way to prepare articuliform tubes. Yarin et al. have found that low molecular weight polymer solutions can enter into carbon nanotubes (CNTs) and form segmented inner structures [93]. They immersed the open-ended CNTs in a dilute solution of low molecular weight polymers, and then the polymers entered into the CNTs and concentrated in the CNTs, driven by a self-sustained diffusion mechanism. As a result, a series of different structured bamboo-like nanotubes were obtained (Figure 13(a)–(c)).

The wire-in-tube micro/nanomaterials are the combination of solid wires and hollow tubes. The wire-in-tube structure is different from core-shell nanowires because there is a void left between the inner wire and the outer tube wall. Knez et al. have fabricated the wire-in-tube nanomaterials by combining atomic layer deposition with the template method [21]. Zussman et al. have produced a kind of polyacrylonitrile/poly (methyl methacrylate) (PAN/PMMA) wire-in-tube structured tube by co-electrospinning. In recent years, co-electrospinning has been a widely used method to fabricate core-shell structured fibers or hollow tubes [94,95]. Zussman et al. used PAN/DMF solution and PMMA/DMF-acetone solution as the shell fluid and the core fluid, respectively [96]. Due to the immiscibility of PAN and acetone, PAN shells rapidly resulted from phase separation at the interface of the PAN and PMMA solution, thus the core PMMA solution incompletely solidified. The volume of PMMA shrank further with subsequent solution evaporation. Therefore, the diameter of the PMMA core is smaller than the inner diameter of the outer PAN tube. The wire-in-tube structured microtubes were obtained (Figure 13(d)).

Multiwalled tubes refer to microscopic tubes with several walls just like the multishell spheres. Yan et al. have synthesized iron single-crystalline hematite tube-in-tube nanostructures by a hydrothermal method, which is shown in Figure 14(a) [97]. In this reaction, they first synthesized solid ellipsoid hematite nanocrystals. The hollowing occurred at both the centered tips of the ellipsoid nanocrystals and several high-energy sites on the top simultaneously. These close proximity holes gradually merged into a continuous void upon increasing the reaction time, and multiwalled structured tubes were obtained.

The self-assembly method is another way to fabricate multiwalled tubes. Yan et al. have reported that multiwalled tubes can be prepared by supramolecular self-assembly [20]. Bo et al. have successfully fabricated rolled-up multiwalled nametapes by hierarchical supramolecular self-assembly of a small organic non-amphiphilic molecule [98]. Yang et al. have synthesized copper chalcogenide nanotubes with double walls by a sacrificial template method (Figure 14(b) and 14(c)) [99].

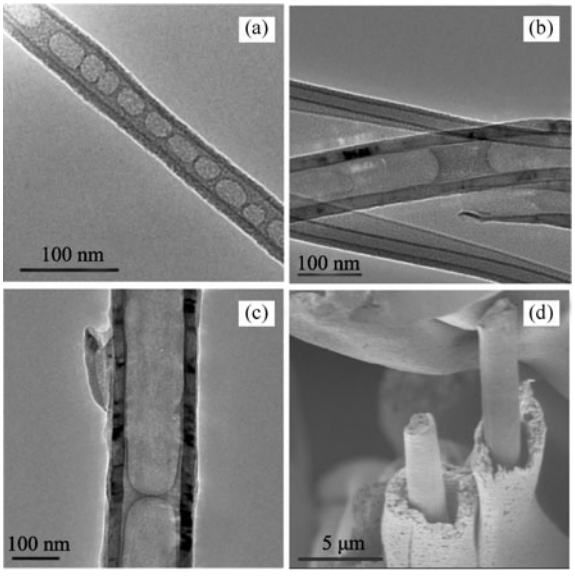

Figure 13 (a)–(c), TEM images of different molecular weight PEO deposits inside CNTs: (a) 600 kDa, (b) 2000 kDa, (c) 4000 kDa. Reprinted with permission from Ref. [93]. Copyright 2007 American Chemical Society. (d) SEM image of broken as-spun core/shell nanofibers [96]. Copyright Wiley-VCH Verlag GmbH & Co. KGaA. Reproduced with permission.

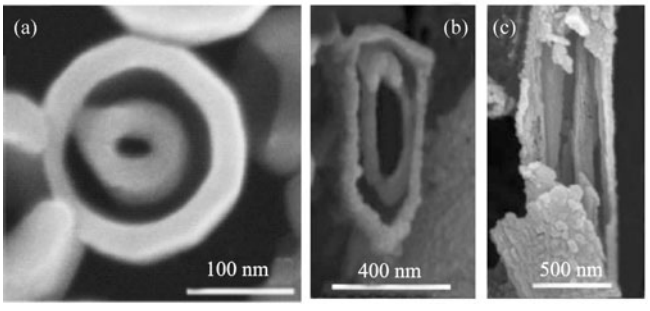

Figure 14 (a) SEM image of the single tube-in-tube nanostructures. Reprinted with permission from Ref. [97]. Copyright 2007 American Chemical Society. (b) and (c): a section view and a side view of a broken double-walled Cu_7S_4 nanotube, respectively. Reprinted with permission from Ref. [99]. Copyright 2007 American Chemical Society.

Multichannel tubes are tubes with multiple independent parallel hollow channels. The side views of the tubes are somewhat like the lotus roots and feathers of some birds. However, due to the hierarchical structure and complicated fabrication route, literature regarding this kind of multi-channel tube is rare. Recently, Jiang et al. reported about a multifluidic compound-jet electrospinning technique that could fabricate hierarchical multichannel microtubes in one

step [18]. The experimental set-up is similar to the above mentioned multifluidic electrospray devices and is shown in Figure 12(a). Two kinds of immiscible viscous liquids, poly (vinyl pyrrolidone)/Ti(iOPr)$_4$ and paraffin, served as shell and core fluids that were fed into the outer nozzle and several inner capillaries separately. After a multifluidic electrospinning process, a piece of large area fibrous film was collected on the grounded substrate below. The multichannel microtubes were obtained upon removing the organics of the as-prepared products by calcination. Figure 15(a)–(d) are the SEM images of the cross section of the multichannel microtubes. The wall thickness and tube diameters can be controlled by adjusting the relative experimental parameters. More importantly, the channel number can also be tuned by changing the configuration of the compound nozzle.

4 Conclusions and outlook

In this review, we have introduced some unique hierarchical structures and special properties in biologic systems. Nature has given us important inspiration in that excellent macroscopic performance can be obtained by mimicking the smart properties of organisms, simulating certain aspects of their special functions and choosing proper materials to create micro/nanostructures. Thereby, the bio-inspired design of advanced materials has become an emerging issue for scientists. We have also summarized some new kinds of 0D and 1D multilevel structured micro/nanomaterials and presented related synthetic methods, related structural properties and some applications. These kinds of multilevel interior structured materials have attracted considerable attention recently due to their complicated structures and amazing properties. Some remarkable features of these micro/nanomaterials include their multilevel interior structures, various chemical compositions, high specific areas, and multiphase anisotropic interfaces. Many kinds of these materials have been generated by scientists in recent years. However, owing to their small size and complicated structures, synthesis routes are not only rather complex, but also not easily controllable. Therefore, the question of how to explore simplicity, quality, and a universal synthesis technique is a challenge for researchers. We believe that multilevel structure micro/nanomaterials will be widely used in energy, environment, medicine, bioengineering and other relative fields in the future.

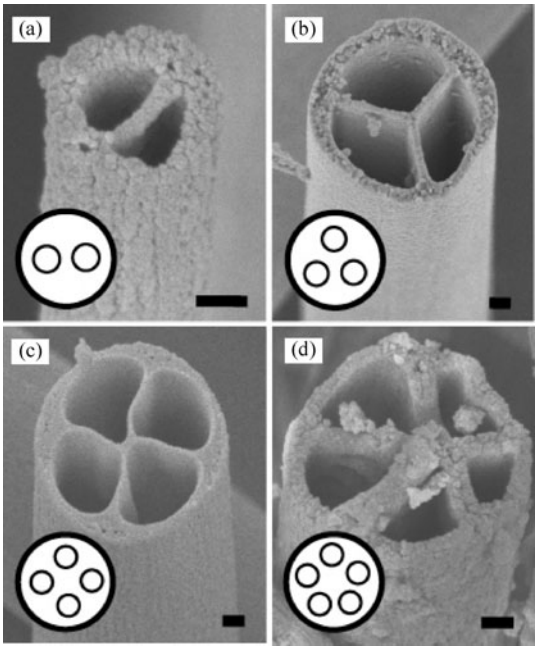

Figure 15 SEM images of multichannel tubes with variable channel numbers. (a)–(d) Corresponding to tube with channel number from two to five. The inset in each figure shows the cross section illustration of spinneret that was used to fabricate the tube. Scale bars are 100 nm. Reprinted with permission from Ref. [18]. Copyright 2007 American Chemical Society.

Acknowledgements The authors would like to thank the support of the National Key Basic Research Special Foundation of China (Grant Nos. 2010CB934700, 2009CB930404, 2007CB936403), the National Natural Science Foundation of China (Grant Nos. 20920102036, 20974113, 20601005, 20801057, 20774101), and Ministry of Science and Technology of China Program (Grant No. 2007AA03Z327).

Nü WANG is currently a lectuer at School of Chemistry and Environment, Beijing University of Aeronautics and Astronautics. She received her B.S. degree from Jilin University of China in 2004, and Ph.D. from the Institute of Chemistry, Chinese Academy of Sciences (ICCAS), China in 2009 (with Prof. Lei Jiang). Her current scientific interests are focused on the functional micro/nanomaterials prepared by electrospinning and their properties.

Yong ZHAO is currently an associate professor at ICCAS. He received his Ph.D. from ICCAS, China in 2007 (with Prof. Lei Jiang). His current scientific interests are focused on the electrostatic force fabrication of multilevelstructured micro/nanomaterials, photocatalysis, and smart multifunctional materials.

Lei JIANG is currently a professor at ICCAS, and Dean of the School of Chemistry and Environment, Beijing University of Aeronautics and Astronautics. He received his B.S. degree (1987), M.S. degree (1990), and Ph.D. degree (1994) from Jilin University of China (Tiejin Li's group). He then worked as a postdoctoral fellow in Prof. Akira Fujishima's group in Tokyo University. In 1996, he worked as a senior researcher in Kanagawa Academy of Sciences and Technology under Prof. Kazuhito Hashimoto. He joined ICCAS as part of the Hundred Talents Program in 1999. His scientific interest is focused on bioinspired surface and interfacial materials.

References

1. Douglas, T., *Science* **2003**, *299*, 1192–1193
2. Taton, T., *Nat. Mater*. **2003**, *2*, 73–74
3. Liu, Y.; Tang, J.; Wang, R.; Lu, H.; Li, L.; Kong, Y.; Qi, K.; Xin, J., *J. Mater. Chem*. **2007**, *17*, 1071–1078
4. Feng, L.; Li, S. H.; Li, Y. S.; Li, H. J.; Zhang, L. J.; Zhai, J.; Song, Y. L.; Liu, B. Q.; et al., *Adv. Mater*. **2002**, *14*, 1857–1860
5. Shi, F.; Niu, J.; Liu, J.; Liu, F.; Wang, Z.; Feng, X. Q.; Zhang, X., *Adv. Mater*. **2007**, *19*, 2257–2261
6. Lee, H.; Lee, B.; Messersmith, P., *Nature* **2007**, *448*, 338–341
7. Watson, G. S.; Watson, J. A., *Appl. Surf. Sci*. **2004**, *235*, 139–144
8. Stavenga, D. G.; Foletti, S.; Palasantzas, G.; Arikawa, K., *Proc. R. Soc. B* **2006**, *273*, 661–667
9. Burda, C.; Chen, X.; Narayanan, R.; El-Sayed, M., *Chem. Rev*. **2005**, *105*, 1025–1102
10. Hodes, G., *Adv. Mater*. **2007**, *19*, 639–655
11. Whitesides, G. M., *Small* **2005**, *1*, 172–179
12. Xia, Y.; Yang, P.; Sun, Y.; Wu, Y.; Mayers, B.; Gates, B.; Yin, Y.; Kim, F.; et al., *Adv. Mater*. **2003**, *15*, 353–389
13. Lou, X. W.; Archer, L. A.; Yang, Z., *Adv. Mater*. **2008**, *20*, 3987–4019
14. Chen, X.; Knez, M.; Berger, A.; Nielsch, K.; Gösele, U.; Steinhart, M., *Angew. Chem. Int. Ed*. **2007**, *46*, 6829–6832
15. Yang, M.; Ma, J.; Zhang, C.; Yang, Z.; Lu, Y., *Angew. Chem. Int. Ed*. **2005**, *44*, 6727–6730
16. Zeng, H. C., *J. Mater. Chem*. **2006**, *16*, 649–662
17. Lou, X. W.; Yuan, C.; Archer, L. A., *Adv. Mater*. **2007**, *19*, 3328–3332
18. Zhao, Y.; Cao, X.; Jiang, L., *J. Am. Chem. Soc*. **2007**, *129*, 764–765
19. Sun, Y.; Xia, Y., *Adv. Mater*. **2004**, *16*, 264–268
20. Yan, D.; Zhou, Y.; Hou, J., *Science* **2004**, *303*, 65–67
21. Qin, Y.; Liu, L.; Yang, R.; Gösele, U.; Knez, M., *Nano Lett*. **2008**, *8*, 3221–3225
22. Zhang, H.; Zhu, Q.; Zhang, Y.; Wang, Y.; Zhao, L.; Yu, B., *Adv. Funct. Mater*. **2007**, *17*, 2766–2771
23. Zhang, W. M.; Hu, J. S.; Guo, Y. G.; Zheng, S. F.; Zhong, L. S.; Song, W. G.; Wan, L. J., *Adv. Mater*. **2008**, *20*, 1160–1165
24. Barthlott, W.; Neinhuis, C., *Planta* **1997**, *202*, 1–8
25. Lum, K.; Chandler, D.; Weeks, J. D., *J. Phys. Chem. B* **1999**, *103*, 4570–4577
26. Gao, X.; Yan, X.; Yao, X.; Xu, L.; Zhang, K.; Zhang, J.; Yang, B.; Jiang, L., *Adv. Mater*. **2007**, *19*, 2213–2217
27. Kennedy, R. J., *Nature* **1970**, *227*, 736–737
28. Zheng, Y.; Gao, X.; Jiang, L., *Soft Matter* **2007**, *3*, 178–182
29. Gao, X.; Jiang, L., *Nature* **2004**, *432*, 36
30. Autumn, K.; Liang, Y.; Hsieh, S.; Zesch, W.; Chan, W.; Kenny, T.; Fearing, R.; Full, R., *Nature* **2000**, *405*, 681–685
31. Eisner, T.; Aneshansley, D., *Proc. Natl. Acad. Sci. U.S.A*. **2000**, *97*, 6568–6573
32. Parker, A.; Lawrence, C., *Nature* **2001**, *414*, 33–34
33. Hadley, N. F., *Science* **1979**, *203*, 367–369
34. Neinhuis, C.; Barthlott, W., *Ann. Bot*. **1997**, *79*, 667–677
35. Feng, L.; Zhang, Y.; Xi, J.; Zhu, Y.; Wang, N.; Xia, F.; Jiang, L., *Langmuir* **2008**, *24*, 4114–4119
36. Shi, F.; Wang, Z.; Zhang, X., *Adv. Mater*. **2005**, *17*, 1005–1009
37. Wu, X.; Shi, G., *J. Phys. Chem. B* **2006**, *110*, 11247–11252
38. Zi, J.; Yu, X.; Li, Y.; Hu, X.; Xu, C.; Wang, X.; Liu, X.; Fu, R., *Proc. Natl. Acad. Sci. U.S.A*. **2003**, *100*, 12576–12578
39. Srinivasarao, M., *Chem. Rev*. **1999**, *99*, 1935–1962
40. Vukusic, P.; Hooper, I., *Science* **2005**, *310*, 1151
41. Vukusic, P.; Sambles, J. R.; Lawrence, C. R.; Wootton, R. J., *Nature* **2001**, *410*, 36
42. Vukusic, P.; Sambles, J.; Lawrence, C., *Nature* **2000**, *404*, 457
43. Parker, A.; Welch, V.; Driver, D.; Martini, N., *Nature* **2003**, *426*, 786–787
44. Yablonovitch, E., *Phys. Rev. Lett*. **1987**, *58*, 2059–2062
45. John, S., *Phys. Rev. Lett*. **1987**, *58*, 2486–2489
46. Aizenberg, J.; Tkachenko, A.; Weiner, S.; Addadi, L.; Hendler, G., *Nature* **2001**, *412*, 819–822
47. Cha, J. N.; Stucky, G. D.; Morse, D. E.; Deming, T. J., *Nature* **2000**, *403*, 289–292
48. Grojean, R.; Sousa, J.; Henry, M., *Appl. Opt*. **1980**, *19*, 339–346
49. Dyck, J., *Zool. Scr*. **1985**, *14*, 137–154
50. Shin, Y.; Wang, C.; Exarhos, G., *Adv. Mater*. **2005**, *17*, 73–76
51. Keckes, J.; Burgert, I.; Fruhmann, K.; Muller, M.; Kolln, K.; Hamilton, M.; Burghammer, M.; Roth, S.; et al., *Nat. Mater*. **2003**, *2*, 810–813
52. He, X. D.; Ge, X. W.; Liu, H. R.; Wang, M. Z.; Zhang, Z. C., *Chem. Mater*. **2005**, *17*, 5891–5892
53. Yang, S.; Liu, H.; Zhang, Z., *Langmuir* **2008**, *24*, 10395–10401
54. Wei, Q.; Wei, W.; Tian, R.; Wang, L. y.; Su, Z. G.; Ma, G. H., *J. Colloid Interface Sci*. **2008**, *323*, 267–273
55. Ma, G. H.; Sone, H.; Omi, S., *Macromolecules* **2004** , *37*, 2954–2964
56. Wei, W.; Wang, L. Y.; Yuan, L.; Wei, Q.; Yang, X. D.; Su, Z. G.; Ma, G. H., *Adv. Funct. Mater*. **2007**, *17*, 3153–3158
57. Wang, R.; Zhang, Y.; Ma, G.; Su, Z., *J. Appl. Polym. Sci*. **2006**, *102*, 5018–5027
58. Zhou, W. Q.; Gu, T. Y.; Su, Z. G.; Ma, G. H.,*Polymer* **2007**, *48*,

1981–1988
59. Zhou, Q. Z.; Wang, L. Y.; Ma, G. H.; Su, Z. G., *J. Colloid Interface Sci*. **2007**, *311*, 118–127
60. Cho, Y. S.; Yi, G. R.; Kim, S. H.; Jeon, S. J.; Elsesser, M. T.; Yu, H. K.; Yang, S. M.; Pine, D. J., *Chem. Mater*. **2007**, *19*, 3183–3193
61. Jiang, L.; Zhao, Y.; Zhai, J., *Angew. Chem. Int. Ed*. **2004**, *43*, 4338–4341
62. Zheng, J. F.; He, A. H.; Li, J. X.; Xu, J. A.; Han, C. C., *Polymer* **2006**, *47*, 7095–7102
63. Li, H.; Wang, H.; Chen, A.; Meng, B.; Li, X., *J. Mater. Chem*. **2005**, *15*, 2551–2556
64. Mai, Y.; Zhou, Y.; Yan, D., *Small* **2007**, *3*, 1170–1173
65. Iskandar, F.; Nandiyanto, A. B. D.; Yun, K. M.; Hogan, C. J. Jr; Okuyama, K.; Biswas, P., *Adv. Mater*. **2007**, *19*, 1408–1412
66. Zhao, Y.; Zhang, X.; Zhai, J.; He, J.; Jiang, L.; Liu, Z.; Nishimoto, S.; Murakami, T.; et al., *Appl. Catal. B* **2008**, *83*, 24–29
67. Salgueiriño-Maceira, V.; Correa-Duarte, M. A., *Adv. Mater*. **2007**, *19*, 4131–4144
68. Zhao, W.; Chen, H.; Li, Y.; Li, L.; Lang, M.; Shi, J., *Adv. Funct. Mater*. **2008**, *18*, 2780–2788
69. Hah, H. J.; Um, J. I.; Han, S. H.; Koo, S. M., *Chem. Commun*. **2004**, 1012–1013
70. Yang, J.; Lu, L.; Wang, H.; Zhang, H., *Scr. Mater*. **2006**, *54*, 159–162
71. Lee, J.; Park, J. C.; Song, H., *Adv. Mater*. **2008**, *20*, 1523–1528
72. Chen, M.; Kim, Y. N.; Lee, H. M.; Li, C.; Cho, S. O., *J. Phys. Chem. C* **2008**, *112*, 8870–8874
73. Gao, J.; Liang, G.; Cheung, J. S.; Pan, Y.; Kuang, Y.; Zhao, F.; Zhang, B.; Zhang, X.; et al., *J. Am. Chem. Soc*. **2008**, *130*, 11828–11833
74. Lou, X. W.; Archer, L. A., *Adv. Mater*. **2008**, *20*, 1853–1858
75. Lou, X. W.; Wang, Y.; Yuan, C.; Lee, J. Y.; Archer, L. A., *Adv. Mater*. **2006**, *18*, 2325–2329
76. Ren, N.; Wang, B.; Yang, Y. H.; Zhang, Y. H.; Yang, W. L.; Yue, Y. H.; Gao, Z.; Tang, Y., *Chem. Mater*. **2005**, *17*, 2582–2587
77. Kamata, K.; Lu, Y.; Xia, Y., *J. Am. Chem. Soc*. **2003**, *125*, 2384–2385
78. Zhang, K.; Zhang, X.; Chen, H.; Chen, X.; Zheng, L.; Zhang, J.; Yang, B., *Langmuir* **2004**, *20*, 11312–11314
79. Liu, G.; Ji, H.; Yang, X.; Wang, Y., *Langmuir* **2008**, *24*, 1019–1025
80. Zhang, T.; Ge, J.; Hu, Y.; Zhang, Q.; Aloni, S.; Yin, Y., *Angew. Chem. Int. Ed*. **2008**, *47*, 5806–5811
81. Zhang, Q.; Zhang, T.; Ge, J.; Yin, Y., *Nano Lett*. **2008**, *8*, 2867–2871
82. Liang, X.; Xu, B.; Kuang, S.; Wang, X., *Adv. Mater*. **2008**, *20*, 3739–3744
83. Li, J.; Zeng, H. C., *J. Am. Chem. Soc*. **2007**, *129*, 15839–15847
84. Liu, B.; Zeng, H. C., *Small* **2005**, *1*, 566–571
85. Yang, H. X.; Qian, J. F.; Chen, Z. X.; Ai, X. P.; Cao, Y. L., *J. Phys. Chem. C* **2007**, *111*, 14067–14071
86. Yang, M.; Ma, J.; Niu, Z.; Dong, X.; Xu, H.; Meng, Z.; Jin, Z.; Lu, Y.; et al., *Adv. Funct. Mater*. **2005**, *15*, 1523–1528
87. Zhou, J.; Chen, M.; Qiao, X.; Wu, L., *Langmuir* **2006**, *22*, 10175–10179
88. Lou, X. W.; Yuan, C.; Archer, L. A., *Small* **2007**, *3*, 261–265
89. Zhao, H.; Chen, J. F.; Zhao, Y.; Jiang, L.; Sun, J. W.; Yun, J., *Adv. Mater*. **2008**, *20*, 3682–3686
90. Nisisako, T.; Okushima, S.; Torii, T., *Soft Matter* **2005**, *1*, 23–27
91. Chu, L. Y.; Utada, A. S.; Shah, R. K.; Kim, J. W.; Weitz, D. A., *Angew. Chem. Int. Ed*. **2007**, *46*, 8970–8974
92. Chen, H. Y.; Zhao, Y.; Song, Y. L.; Jiang, L., *J. Am. Chem. Soc*. **2008**, *130*, 7800–7801
93. Bazilevsky, A. V.; Sun, K.; Yarin, A. L.; Megaridis, C. M., *Langmuir* **2007**, *23*, 7451–7455
94. Li, D.; Xia, Y., *Nano Lett*. **2004**, *4*, 933–938
95. Loscertales, I. G.; Barrero, A.; Guerrero, I.; Cortijo, R.; Marquez, M.; Ganan-Calvo, A. M., *Science* **2002**, *295*, 1695–1698
96. Zussman, E.; Yarin, A. L.; Bazilevsky, A. V.; Avrahami, R.; Feldman, M., *Adv. Mater*. **2006**, *18*, 348–353
97. Jia, C. J.; Sun, L. D.; Yan, Z. G.; Pang, Y. C.; You, L. P.; Yan, C. H., *J. Phys. Chem. C* **2007**, *111*, 13022–13027
98. Chen, Y.; Zhu, B.; Zhang, F.; Han, Y.; Bo, Z., *Angew. Chem. Int. Ed*. **2008**, *47*, 6015–6018
99. Xu, J.; Zhang, W.; Yang, Z.; Yang, S., *Inorg. Chem*. **2008**, *47*, 699–704